Carnegie Observatories Astrophysics Series, Vol. 3:
Clusters of Galaxies: Probes of Cosmological Structure and Galaxy Evolution, 2004
ed. J. S. Mulchaey, A. Dressler, and A. Oemler (Pasadena; Carnegie Observatories:
http://www.ociw.edu/ociw/symposia/series/symposium3/proceedings.html)

The Mass Profile of Clusters from ENACS

A. BIVIANO[1], P. KATGERT[2], and A. MAZURE[3]
(1) INAF-Osservatorio Astronomico di Trieste, Trieste, Italy
(2) Sterrewacht Leiden, Leiden, The Netherlands
(3) OAMP, LAM, Marseille, France

Abstract

We determine the mass profile of an ensemble cluster built from a sample of 59 nearby clusters observed in the ESO Nearby Abell Cluster Survey (ENACS), for which galaxy morphologies were recently determined. The shape of the velocity distribution of ellipticals and S0s (with $M_R > -22.8$) suggests we can use these galaxies as tracers of the cluster potential on isotropic orbits. We solve the Jeans equation to determine the cluster mass profile and find it to be consistent with the Navarro, Frenk & White model, as well as with the model suggested by Moore et al. A softened isothermal sphere model is rejected by our data, unless the core radius of the mass profile is very small, of order of the size of a galaxy. The cluster mass-to-luminosity density profile is nearly constant with radius, when only ellipticals and S0s are considered. However, the luminosity density of bright ($M_R \leq -22.8$) ellipticals is more concentrated, and those of early- and late-type spirals are less concentrated, than the total cluster mass density. Finally, we determine the velocity-anisotropy profiles of early- and late-type spirals.

1.1 Introduction

Knowledge of the mass distribution within clusters, and of the relative distribution of mass and light is crucial for our understanding of the formation and evolution of galaxy clusters. Cosmological simulations have shown that dark matter halos have a universal density profile (Navarro, Frenk & White 1997, NFW herafter), although the precise form of it is still uncertain (Moore et al. 1999, M99), and may depend on the mass of the system (Ricotti 2003).

Recent results obtained from optical, X-ray, and gravitational lensing analyses, generally indicate consistency with the NFW (or, in some cases, the M99) profile (see, e.g., Arabadjis, Bautz, & Garmire 2002; Biviano & Girardi 2003; Clowe & Schneider 2001; Geller, Diaferio, & Kurtz 1999; Rines et al. 2000, 2002; van der Marel et al. 2000), but flatter mass profiles are still preferred in several clusters (see, e.g., Ettori, De Grandi & Molendi 2002; Kelson et al. 2002; Sand, Treu & Ellis 2002). Also cluster total-to-baryonic mass-profiles are still very uncertain. Generally, the intra-cluster gas is found to be less concentrated than the total cluster mass (see, e.g, Markevitch & Vikhlinin 1997; Pratt & Arnaud 2002), while the mass-to-optical light profile has been found to be flat (see, e.g., Carlberg, Yee, & Ellingson 1997; Hoekstra et al. 2002; Rines et al. 2001; van der Marel et al. 2000), decreasing (Rines et al. 2000), as well as increasing (Carlberg et al. 2001), depending on the photometric band, the membership selection, or the cluster population considered (see, e.g. Biviano & Girardi 2003).

Here we present a new analysis of the cluster mass profile, based on optical data for about 3000 galaxies in 59 clusters obtained in the ESO Nearby Abell Cluster Survey (ENACS, Katgert et al. 1996, 1998). This is the largest spectroscopic sample of cluster galaxies currently available, allowing us to put strong constraints on the average cluster mass profile, and also to explore the orbital anisotropy profiles of different cluster galaxy populations.

1.2 The Data

We base our analysis on the ENACS data-set, complemented by spectral-type and new morphological data (Thomas & Katgert 2004). We have positions, redshifts, and spectral or morphological types for nearly 3000 member galaxies in 59 nearby clusters ($z < 0.1$). We assign the cluster membership based on the algorithm of den Hartog & Katgert (1996; see Biviano et al. 2002, B02 hereafter, for details). We combine these 59 clusters into an ensemble cluster by scaling the projected clustercentric distances of individual galaxies with r_{200} (Carlberg et al. 1997), and the galaxy velocities (relative to the cluster mean) with the total cluster line-of-sight velocity dispersion σ_p.

In B02 it was found that galaxies in substructure have different phase-space distributions from those outside substructure. The analysis of the mass profile cannot be based on the sample of galaxies within substructure because the kinematics of these galaxies enters the very definition of subclusters. We therefore exclude galaxies in substructure from our sample. We are thus left with ~ 2200 galaxies, which we split into four populations because they have significantly different phase-space distributions (see B02): (i) the "*Bright*' population, i.e. very bright ellipticals (with $M_R \leq -22.8^*$), (ii) the '*Early*' population, i.e. fainter ellipticals together with E/S0s and S0s, (iii) the "*S-early*' population, i.e. early spirals (Sa–Sb), and (iv) the "*S-late*' population, i.e. late spirals, irregulars (Sbc–Ir) and emission-line galaxies (except those with early morphology).

1.3 Analysis

1.3.1 The Mass Profile

In order to determine the cluster mass profile from the projected distributions of galaxy positions and velocities, we solve the spherically-symmetric† Jeans equation (see, e.g., Binney & Tremaine 1987) for the *Early* population of cluster galaxies, that we adopt as our *bona-fide* tracers of the cluster potential, since they are the dominant and probably the oldest cluster population.

Knowledge of the velocity-anisotropy profile, $\beta(r) \equiv 1-(\overline{v_t^2}/\overline{v_r^2})$‡, is required in order to solve for the mass profile. Useful constraints on $\beta(r)$ can be obtained by the analysis of the shape of the velocity distribution of the galaxy population (e.g. Merritt 1987; van der Marel et al. 2000). We use the Gauss-Hermite moments to parametrize the shape of the *Early* population velocity distribution. By comparing the values of the Gauss-Hermite moments

* We use $H_0 = 70$ km s^{-1} Mpc^{-1} in this paper.

† Although galaxy clusters are not spherically symmetric (see, e.g., de Theije, Katgert, & van Kampen 1995), the ensemble cluster is spherical by construction.

‡ $\overline{v_t^2}$ and $\overline{v_r^2}$ are the mean square components of the tangential and radial velocity, respectively. We implicitely assume in our analysis that the two mean squared components of the tangential velocity are identical.

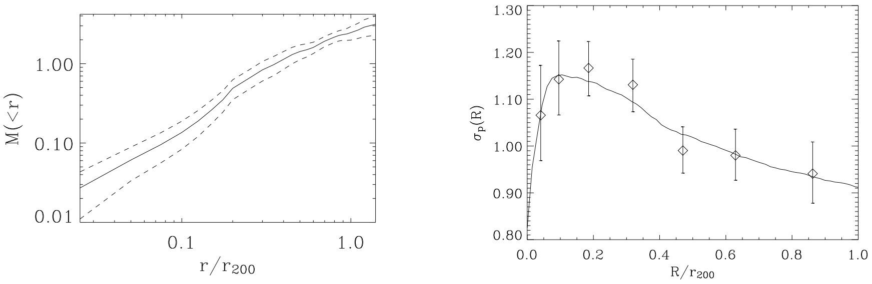

Fig. 1.1. Left panel: The mass profile of the ensemble cluster (solid line). Dashed lines indicate the 68% confidence levels. The mass scale is in normalised units. Right panel: the observed velocity dispersion profile of the *Early* population (diamonds with 68% error bars), and the best-fit model velocity dispersion profile for the NFW mass profile, $r_s/r_{200} = 0.25$ (solid line).

with those of constant-anisotropy models built by van der Marel et al. (2000), we infer $(\overline{v_r^2}/\overline{v_t^2})^{1/2} \simeq 1.0$ to within 15%, i.e. $\beta \approx 0$.

We therefore assume $\beta \equiv 0$ for the *Early* population, and solve the isotropic Jeans equation. We first determine the projected number density and velocity dispersion profiles of the *Early* galaxies non-parametrically, using the LOWESS algorithm (Gebhardt & Fischer 1995), and then deproject these profiles via the usual Abel inversion. The resulting mass profile $M(<r)$ is shown in Figure 1.1, left panel (the mass scale is in normalised units*). The 68% confidence levels (c.l., hereafter) are obtained from a bootstrap analysis.

In order to compare our solution with popular models, we work in the domain of observables, i.e. the projected velocity dispersion profile, $\sigma_p(R)$. We do this by inverting the isotropic Jeans equation to derive $\sigma_p(R)$ per given mass profile $M(<r)$, as described by van der Marel (1994). We consider three models: those of NFW and M99, and the softened isothermal sphere (SIS, hereafter). All three models provide acceptable fits to our data, although NFW and M99 models are marginally better. We show in Figure 1.1, right panel, the observed $\sigma_p(R)$ for the *Early* cluster galaxy population, and the best-fit model $\sigma_p(R)$ for the NFW mass profile. The best-fit value of the NFW and M99 scale parameters are $r_s/r_{200} = 0.25^{+0.15}_{-0.10}$ and $r_M/r_{200} = 0.5^{+0.20}_{-0.15}$, respectively (68% c.l.). On the other hand, for no value of the scale parameter r_c is the SIS model acceptable at the 68% c.l. (or better). The best-fit is obtained for $r_c/r_{200} = 0.025$, and values $r_c/r_{200} > 0.075$ are rejected at $> 99\%$ c.l.

1.3.2 The Mass-to-Light Density Profiles

In order to build the mass-to-light density profile, ρ/l, we divide the best-fit mass density model (i.e. NFW with $r_s/r_{200} = 0.25$) by the luminosity density profiles of the four cluster galaxy populations, separately. By comparing the *total* mass density profile to the luminosity density profile of each given population, we investigate whether any of the four cluster galaxy populations is an unbiased tracer of the mass. The 68% c.l. on ρ/l are obtained by taking into consideration the (NFW and M99) mass density models that provide

* From the average σ_p of the 59 clusters in our sample, we estimate that one mass unit corresponds to $\sim 2 \cdot 10^{14} M_\odot$.

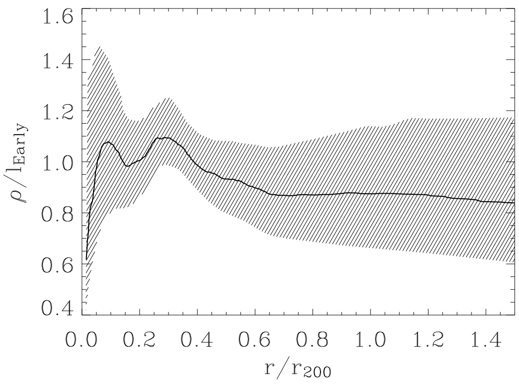

Fig. 1.2. The ratio of the total cluster mass density profile to the luminosity density profile of the *Early* cluster galaxy population. The solid line is obtained using the $r_s/r_{200} = 0.25$ NFW mass density model, and the hatched region indicate the 68% c.l. The vertical scale is in relative units.

acceptable fit to our data (at the 68% c.l.; see § 1.3.1). We find that the luminosity density profile of the *Early* population is similar to the mass density profile, i.e. ρ/l_{Early} is roughly constant for $r/r_{200} \leq 1.5$ (see Figure 1.2). On the other hand, this is not the case for other cluster populations. In particular, ρ/l_{Bright} significantly increases with radius, while both $\rho/l_{S\text{–}early}$ and $\rho/l_{S\text{–}late}$ decrease with radius.

1.3.3 The Velocity-Anisotropy Profiles

Using the cluster mass profile determined from the *Early* class (see § 1.3.1), we search for equilibrium solutions for the other three classes of cluster galaxies. For this, we solve the anisotropic Jeans equation using the method of Solanes & Salvador-Solé (1990).

We do not find an acceptable equilibrium solution for galaxies of the *Bright* class. A possible interpretation of this result is that *Bright* galaxies in clusters are subject to dissipative processes, such as mergers and dynamical friction, affecting their phase-space distribution (see Menci & Fusco-Femiano 1996), so that the use of the *collisionless* Jeans equation is not warranted in this case. We do find equilibrium solutions for both the *S-early* and the *S-late* populations. The isotropic solution is acceptable for the *S-early* population, but is rejected for the *S-late* population. However, in both cases the best agreement between the data and the mass model is obtained for partly radially-anisotropic profiles. The velocity-anisotropy of *S-early* galaxies reaches a maximum $\beta \simeq 0.7$ at $r/r_{200} \simeq 0.4$, and then rapidly decreases at larger radii. On the other hand, the velocity-anisotropy profile of *S-late* galaxies monotonously increases from $\beta \sim 0$ at $r/r_{200} \simeq 0.6$, to $\beta \sim 0.6$ at the limiting radius of our sample, $r/r_{200} = 1.5$.

1.4 Conclusions

Based on ENACS data, supplemented with new galaxy morphology data, we determine the mass profile of galaxy clusters, using galaxies of the *Early* class as tracers of the cluster gravitational potential. By the analysis of the velocity distribution of *Early* galaxies, we show that they are on nearly isotropic orbits.

Among three popular models of cluster mass density profiles, we find that the NFW model with a scale parameter $r_s/r_{200} = 0.25^{+0.15}_{-0.10}$ provides the best-fit to our data. The SIS model is ruled out for core-radii greater than $0.075\, r_{200}$.

Galaxies of the *Early* class are unbiased tracers of the mass distribution, as shown by the similarity of their luminosity density profile and the total cluster mass density profile. On the other hand, the luminosity density of galaxies of the *Bright* class is more concentrated, and those of the *S-early* and *S-late* classes are less concentrated, than the cluster mass density.

While galaxies of the *Early* class are on nearly isotropic orbits, galaxies of the *S-late* class have increasingly radial velocity anisotropy with increasing distance from the cluster center. Although we cannot rule out isotropic orbits for the *S-early* class galaxies, the data taken at face value suggest that they also have a moderate radial velocity-anisotropy, reaching a maximum at intermediate cluster distances. Finally, the fact that we do not find acceptable equilibrium solutions for the galaxies of the *Bright* class, points to the need of including collisional processes in the description of the dynamics of this population of cluster galaxies.

References

Arabadjis, J. S., Bautz, M. W., & Garmire, G. P. 2002, ApJ, 572, 66

Binney, J. & Tremaine, S. 1987, Galactic Dynamics (Princeton: Princeton University Press)

Biviano, A. & Girardi, M. 2003, ApJ, 585, 205

Biviano, A., Katgert, P., Thomas, T., & Adami, C. 2002, A&A, 387, 8 (B02)

Carlberg, R. G., Yee, H. K. C., Ellingson, E. 1997, ApJ, 478, 462

Carlberg, R. G., Yee, H. K. C., Morris, S. L., Lin, H., Hall, P. B., Patton, D. R., Sawicki, M., & Shepherd, C. W. 2001, ApJ, 552, 427

Clowe, D. & Schneider, P. 2001, A&A, 379, 384

den Hartog, R., & Katgert, P. 1996, MNRAS, 279, 349

de Thejie, P.A.M., Katgert, P., & van Kampen, E. 1995, MNRAS, 274, 975

Ettori, S., De Grandi, S., & Molendi, S. 2002, A&A, 391, 841

Gebhardt, K., & Fischer, P. 1995, AJ, 109, 209

Geller, M. J., Diaferio, A., & Kurtz, M. J. 1999, ApJ, 517, L23

Hoekstra, H., Franx, M., Kuijken, K., & van Dokkum, P. G. 2002, ApJ, 577, 604

Katgert, P., et al. 1996, A&A, 310, 8

Katgert, P., Mazure, A., den Hartog, R., Adami, C., Biviano, A., & Perea, J. 1998, A&A, 129, 399

Kelson, D. D., Zabludoff, A. I., Williams, K. A., Trager, S. C., Mulchaey, J. S., & Bolte, M. 2002, ApJ, 576, 720

Markevitch, M., & Vikhlinin, A. 1997, ApJ, 491, 467

Menci, N., & Fusco-Femiano, R. 1996, ApJ, 472, 46

Merritt, D. 1987, ApJ, 313, 121

Moore, B., Quinn, T., Governato, F., Stadel, J., & Lake, G. 1999, MNRAS, 310, 1147 (M99)

Navarro, J., Frenk, C. & White, S. D. M. 1997, ApJ, 490, 493 (NFW)

Pratt, G. W., & Arnaud, M. 2002, A&A, 394, 375

Ricotti, M. 2003, MNRAS, 344, 1237

Rines, K., Geller, M. J., Diaferio, A., Mohr, J. J., & Wegner, G. A. 2000, AJ, 120, 2338

Rines, K., Geller, M. J., Kurtz, M. J., Diaferio, A., Jarrett, T. H., & Huchra, J. P. 2001, ApJ, 561, L41

Rines, K., Geller, M. J., Diaferio, A., Mahdavi, A., Mohr, J. J., & Wegner, G. 2002, AJ, 124, 1266

Sand, D. J., Treu, T., & Ellis, R. S. 2002, ApJ, 574, L129

Solanes, J. M. & Salvador-Solé, E. 1990, A&A, 234, 93

Thomas, T. & Katgert, P. 2004, in preparation

van der Marel, R. 1994, MNRAS, 270, 271

van der Marel, R., Magorrian, J., Carlberg, R., Yee, H., & Ellingson, E. 2000, AJ, 119, 2038